Structure, surface topography and optical characterization of Ag co – doped $Cd_{1-x}Cu_xO$ nanostructure thin films

Adel H. Omran Alkhayatt

Physics Department, Faculty of Science, University of Kufa, Najaf, Iraq.
adilh.alkhayat@uokufa.edu.iq

Abstract:

$Cd_{1-x}Cu_xO$ and Ag co-doped $Cd_{1-x}Cu_xO$ nanostructure thin films with x = 0.2 and different Ag content (0-8%) were deposited by chemical spray pyrolysis technique on glass substrates at a temperature of 350 ^oC. The XRD results showed that the prepared films have polycrystalline with low crystallinity nature for CdO cubic structure. The preferential orientation of all films was absorbed along (111) plane. CuO monoclinic phase has appeared with low intensity while the Ag cubic phase appeared only in 8% of Ag content. Structural parameters such as average crystallite size, dislocation density and micro-strain were also investigated. SEM images revealed that the surface morphology of the films consists of spherical shaped grains uniformly distributed without detectable micro-cracks and improved by Ag Co-doping. EDXS spectrum analysis confirmed purity and stoichiometry of the prepared compositions. AFM results showed that the surface topography and the surface quality of the deposited thin films can be controlled by the variation of the Ag co-doping concentration. Optical absorbance and transmittance of Ag co-doped $Cd_{1-x}Cu_xO$ thin films has high values in the visible and near infrared regions respectively and varied with Ag co-doping content. Direct optical energy band gap of $Cd_{1-x}Cu_xO$ exhibits a blue shift with Ag co-doping, due to the quantum size and Burstein–Moss (BM) effects. The increasing of optical energy gap was confirmed by the decrease in the Urbach tails energy E_U after Ag co-doping..

Keywords: Ag co-doped Cd1-xCuxO ; Thin films; TCO; Structural and optical properties; Surface Topography.

توصيف الخصائص التركيبية وطبوغرافية السطح والبصرية لأغشية $Cd_{1-x}Cu_xO$ نانوية التركيب ثنائية التطعيم بالفضة

عادل حبيب عمران الخياط

قسم الفيزياء، كلية العلوم، جامعة الكوفة، النجف، العراق.

الخلاصة:

أغشية $Cd_{1-x}Cu_xO$ و أغشية $Cd_{1-x}Cu_xO$ نانوية التركيب الرقيقة ثنائية التطعيم بالفضة رسبت بواسطة تقنية الانحلال الحراري الكيميائي على قواعد زجاجية عند درجة حرارة 350 درجة مئوية. وأظهرت نتائج حيود الأشعة السينية أن الأغشية المحضرة ذات تركيب متعدد التبلور وبطبيعة تبلور منخفضة. الاتجاه التفضيلي للتبلور لجميع الأفلام على طول المستوي (111). وقد ظهر طور أحادي الميل لأوكسيد النحاس وبشدة حيود منخفضة في حين أن طورالفضة المكعب ظهر فقط عند 8٪ فضة من المحتوى. كما تم أيضا دراسة المعاملات التركيبية مثل متوسط حجم البلورات، وكثافة

الأنحلاعات والمطاوعة المايكروية. كشفت صور المجهر الألكتروني الماسح أن مورفولوجيا سطح الأغشية تتكون من حبوب كروية الشكل موزعة بشكل متجانس مع عدم وجود الشقوق الصغيرة وتحسينها بالتشويب الثنائي بالفضة. أكد تحليل الطيف EDXS نقاوة والنسب الكيميائية المتكافئة للمركبات المحضرة. وأظهرت نتائج مجهر القوة الذرية أن تضاريس وجودة السطح للأغشية الرقيقة المحضرة يمكن السيطرة عليها من خلال تغيير تركيز شائبة الفضة الثنائية. الامتصاصية والنفاذية البصرية لأغشية $Cd_{1-x}Cu_xO$ ثنائية التطعيم بالفضة لها قيم عالية في المنطقة المرئية والمنطقة تحت الحمراء القريبة على التوالي وتتغير مع تغير محتوى التطعيم الثنائي بالفضة. فجوة الطاقة البصرية المباشرة لأغشية $Cd_{1-x}Cu_xO$ تظهر ازاحة زرقاء بالتشويب الثنائي بالفضة، وذلك بسبب الحجم الكمي و تأثير B-M. وقد تأكدت زيادة فجوة الطاقة البصرية من خلال الانخفاض في طاقة ذيول أورباخ بعد التشويب الثنائي بالفضة.

الكلمات المفتاحية:التطعيم الثنائي Cd1-xCuxO بالفضة ; أغشية رقيقة ;TCO; الخصائص التركيبية والبصرية; طبوغرافية السطح.

1. Introduction

(TCOs) Transparent conducting oxides materials attracted great attention due to its unique optical and electrical properties which can be controlled by doping with different metallic ions. Cadmium oxide CdO is one of the n-type TCOs belonging to the II-VI group with high conductivity $\approx 10^2–10^4$ $(\Omega\ cm)^{-1}$ and high transparency in the visible region. The CdO direct band gap is in the range of 2.2-2.5 eV [1-4]. Therefore doped CdO films were suitable in wide range of optoelectronic applications such as photo-transistors, photo-diodes, photo detector, photovoltaic cells, gas sensors, transparent electrodes, IR reflectors, liquid crystal displays and anti-reflection coating [1, 2, 5, 6]. Several techniques were used to preparation of pure and doped CdO thin films such as thermal evaporation [4], high vacuum successive thermal deposition [2], successive ionic layer (silar method) [3], DC reactive magnetron sputtering [5], sol–gel method [7,8], electrochemical deposition [9] vapor transport process (solid–vapor deposition)[10], PLD [11], CBD method [12,13] and chemical spray pyrolysis method [6,14].

The structural, morphological and optical properties of CdO can be modify and control by doping with metallic ions. It is reported that doping CdO with smaller size metallic ions than Cd^{+2} such as Cu, Fe, Sn and In [2, 3, 8]. Sn, In and fluorine doped CdO blue shifted its absorption edge (band gap increases), decreased in the electrical conductivity and changes in the structural and morphological properties [15,16,17]. While the absorption edge red shifted (band gap decreases) and increases in the electrical conductivity with increase Cu, Al and Ag doping level and when CdO doped with larger size metallic ions such as Ag [3, 18, 19,20].

In this study, for the first time we report the synthesis and structural, morphological, optical properties of Ag co-doped $Cd_{1-x}Cu_xO$ thin films by chemical spray pyrolysis method.

2. Experiment details

Thin films of Ag co-doped $Cd_{1-x}Cu_xO$ were deposited on glass substrates at 350 ^oC using spray pyrolysis technique on glass .0.1 M concentration of $Cd(NO_3)_2.4H_2O$ (Mw:308.48), $Cu(NO_3)_2.3H_2O$ (Mw:241.60) and $AgNO_3$ (Mw: 169.873) solutions were used as a starting materials. In the Cu doped CdO ($Cd_{1-x}Cu_xO$) thin film the Cu^{2+} concentration was fixed at a pre-determined value x = 0.2 for all portions, where x represent the molar concentration in the spraying solution. For Ag co-doped $Cd_{1-x}Cu_xO$ the molar concentration values of Ag^{2+} was (4, 6 and 8 %) from the total

solution volume. The starting materials were dissolving in distilled water and mixed by magnetic stirrer for 10 min. The starting solutions is sprayed onto microscopic glass slides substrates with dimensions of 2.5 × 2.5 cm^2 after it ultrasonically cleaned in distilled water, acetone and absolute ethanol. The optimum conditions of the deposition parameters were kept constant, such as substrate spray nozzle distance (30 cm), spray time (15 s), spray interval (3 min.), carrier gas pressure (compressed air – 50 kg/cm^2) and flow rate of the solution (_8 ml/min). The possible chemical reactions that take place on the heated substrate to produce CdCuO and Ag:CdCuO films may be as follows:

$$Cd(NO3)_2 + Cu(NO3)_2 \xrightarrow{\text{decomposition at } 350\ ^oC} CdCuO + NO_2 \uparrow + O_2 \uparrow$$

$$Cd(NO3)_2 + Cu(NO3)_2 + Ag\,NO_3 \xrightarrow{\text{decomposition at } 350\ ^oC} CdCuO{:}Ag + NO_2 \uparrow + O_2 \uparrow$$

The films thickness was found about 250 nm measured by using optical thin measurement model LIMF-10 by Lambda Scientific, Ltd. Company. The structural properties of the prepared films were studied by XRD-6000 Shimadzu diffractometer using CuKα radiations (λ 1.5406Å). SEM (INSPECT- 550) was normally performed at 10 kV to measure the surface morphology of the samples. In most cases, the magnifications were set at 2 μm. Atomic Force Microscopy studies were recorded by using a CSPM model AA3000 AFM. The optical absorption and transmittance spectra are recorded at 200–1100 nm wavelength using a SCINCO Mega 2100 Pc UV– VIS spectrophotometer at room temperature.

3. Result and Discussion:

3.1 Structural characteristics

The structure properties of Ag co-doped $Cd_{1-x}Cu_xO$ have been investigated by XRD. The diffraction pattern shows that all samples have polycrystalline with low crystallinlty nature of cubic CdO structure as depicted in fig. 1, with lattice constant about (4.6836 Å) which is very close to the JPCDS value (4.6953 Å). The preferred orientation (111), (200), (220) and (311) are observed at two theta equal to 33.1011^o, 38.4417^o, 55.4759^o, and 66.2057^o respectively. The diffraction peaks can correspond to the absorbed peaks for cubic CdO (JCPDS Card no.: 01-1049).The monoclinic structure of CuO phase has appeared with low intensity at two theta 35.5674^o of (002) plane which well corresponding to the monoclinic CuO (JCPDS Card no.:02-1040). The low intensity can be attributed to the high intensity of cubic CdO phase as shown in fig.1 a. Where the Cu ions (20%) highly doped CdO thin film with smaller size of dopant Cu^{+2} ions (87 pm) [15] comparing to that of Cd^{+2} (109 pm) [3, 15] lead to replacement of Cd ions by Cu ions in the CdO lattice. Similar results were observed by different studies [4, 21, 22]. After co-doping with (4,6 and 8 %) molar percentage ratios with larger size (115 pm) [3,15] of Ag ion comparing to that of Cd^{+2} the intensity of CdO preferential orientations peaks (111), (200) decreases with increasing of Ag percentage ratio so the CuO phase peak appears with clear height as shown in fig.1 (b,c and d). The lowering of the peaks intensity after Ag co-doped CdCuO thin films may be attributed that the Ag ions replaced the oxygen ions in the CdCuO lattice. Furthermore, at higher Ag percentages, apart from replacing the oxygen ions, Ag ions might occupy the interstitial positions in the CdCuO lattice. These results were in good agreement with literature [3,20,21,23]. It

is obvious from fig.1d that the Ag cubic phase appears with a low intensity only at higher percentage ratio of Ag dopant at two theta 43.8414^{o} of (200) plane which is corresponding to cubic Ag (JCPDS card no.:04-0783).

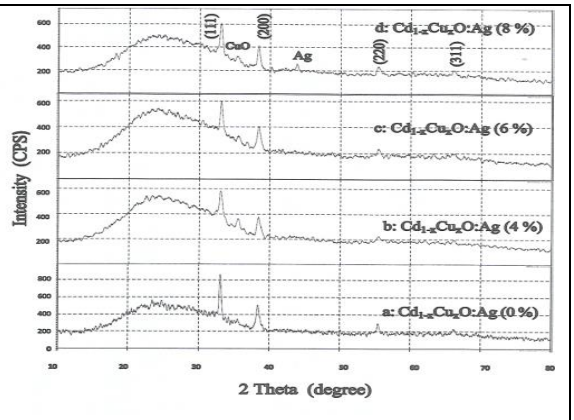

Fig. 1: XRD pattern of Ag co-doped $Cd_xCu_{1-x}O$ thin films.

The structural parameters such as lattice constant average grain size (D), dislocation density (δ), the number of crystallites per unit surface area (N) and micro-strain (ε) were calculated from the XRD data. The calculated lattice constant a are tabulated in table 1 which are in a good agreement with the reported value in (JCPDS Card). The crystallite size for the preferential orientations of the prepared samples was calculated using Debye-Sherrer formula [24,25].

$$D = \frac{0.9\lambda}{B\cos\theta} \qquad (1)$$

Where λ is the wavelength of the x-ray (1.5406 Å), θ is Bragg angle and B is the FWHM (full width at half maximum) value in radian .The variation of the crystallite size as a function of Ag co-doped percentage shown in fig. 2. The calculated crystallite size D for (111) plane of $Cd_{1-x}Cu_xO$ is found to be decreased from 21.59 nm to 18.35 nm and to 17.59 for 4% and 6% Ag co-doped $Cd_{1-x}Cu_xO$ respectively then it increase to 19.86 nm with increase of Ag o-doped percentage to 8 % as shown in table 1. This variation in the crystallite size value indicate that the Ag dopant was contributed in the crystallinty change furthermore the preferred growth orientation of $Cd_{1-x}Cu_xO$. The dislocation density (δ) which can be defined as the dislocation line per unit volume, were calculated using the relation [26].

$$\delta = \frac{1}{(D)^2} \qquad (2)$$

The measurement of the dislocation density (δ) quantifies the count of the defects presented in crystalline thin films. The small value of (δ) obtained in the present work confirms that the spray pyrolysis is an effective technique can be used to deposit good and high quality Ag co-doped $Cd_{1-x}Cu_xO$ thin films [26.27].

The number of crystallites per unit surface area (N) could be calculated using the relation [28.29]:

$$N = \frac{t}{(D)^3} \qquad (3)$$

Where t is the thickness of the films. The variation of (δ) and (N) as a function of Ag co-dopant concentration shown in figure 3, it is absorbed that (N) has the same behavior of (δ) were they increasing with decreasing crystallite size and with the increasing of Ag co-doped concentration up to 6% of Ag dopant concentration then it decreases for 8% Ag co-doping concentration. The calculated values of (δ) and (N) shown in table 1.

The micro-strain (ε) has been determined using the following equation [26, 30]:

$$\text{Micro\_Strain } (\varepsilon) = \frac{B\cos\theta}{4} \qquad (4)$$

The variation of micro-strain (ε) as a function of Ag co-doped $Cd_{1-x}Cu_xO$ concentration for (111) and (200) plans

shown in figure 4. It is notice that the micro-strain exhibits an increasing with increasing Ag co-dopant concentration up to 6% then it also decreases for 8% Ag co-doping concentration. The type of micro-strain changes can be attributing to the crystallization process in polycrystalline thin films.

Table 1: Structural parameters of Ag co-doped $Cd_{1-x}Cu_xO$ thin films obtained from XRD data as a function of Ag doping concentration.

Diffraction plane	Ag Co-doped $Cd_{1-x}Cu_xO$ ratio	2Θ Degree	Lattice Constant a (Å)	FWHM	Crystallite Size (nm)	Dislocation density (δ) 10^{15}lines/m^2	(N) 10^{16} m^{-2}	Micro-strain (ε) 10^{-3}
(111)	0%	33.101	4.6836	0.3307	21.59	2.15	1.24	1.382
	4%	33.077	4.6869	0.4750	18.35	2.97	2.02	1.986
	6%	33.123	4.6806	0.4920	17.59	3.23	2.30	2.058
	8%	33.049	4.6907	0.4360	19.86	2.54	1.60	1.823
(200)	0%	38.441	4.7664	0.4800	17.37	3.31	2.39	1.976
	4%	38.435	4.6804	0.5200	16.90	3.50	2.59	2.141
	6%	38.445	4.6793	0.5600	15.70	4.06	3.23	2.306
	8%	38.362	4.6888	0.3750	23.44	1.82	0.971	1.545

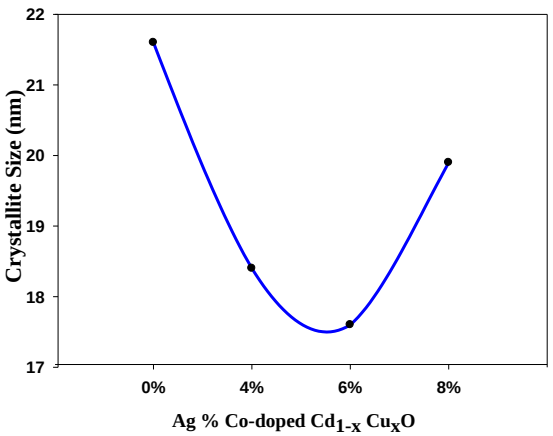

Fig. 2: Variation of the crystallite size of Ag co-doped $Cd_{1-x}Cu_x$Othin films for (111) plane as a function Ag dopant concentration.

D

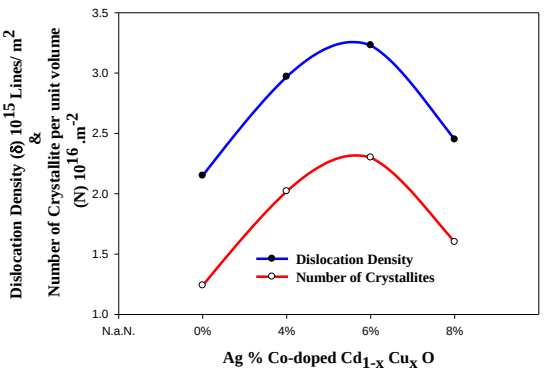

Fig.3: The variation of (δ) and (N) as a function of Ag co-doped $Cd_{1-x}Cu_xO$ concentration for (111) plane.

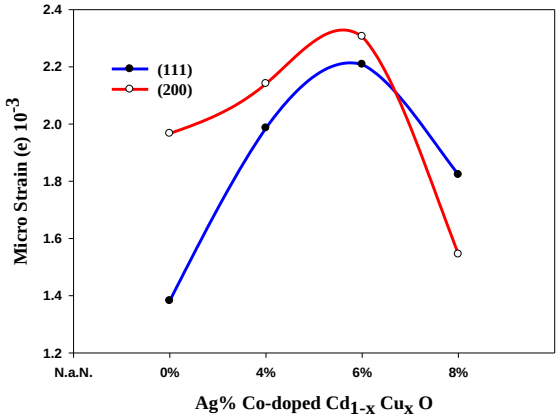

Fig. 4: The variation of micro-strain (ε) as a function of Ag co-doped $Cd_{1-x}Cu_xO$ concentration for (111) and (200) plans.

3.2 Surface morphology & EDXS analysis

The surface morphology and the surface microstructure of Ag co-doped $Cd_{1-x}Cu_xO$ as a function of Ag dopant concentration obtained from SEM is illustrated in fig.5 (a-d).

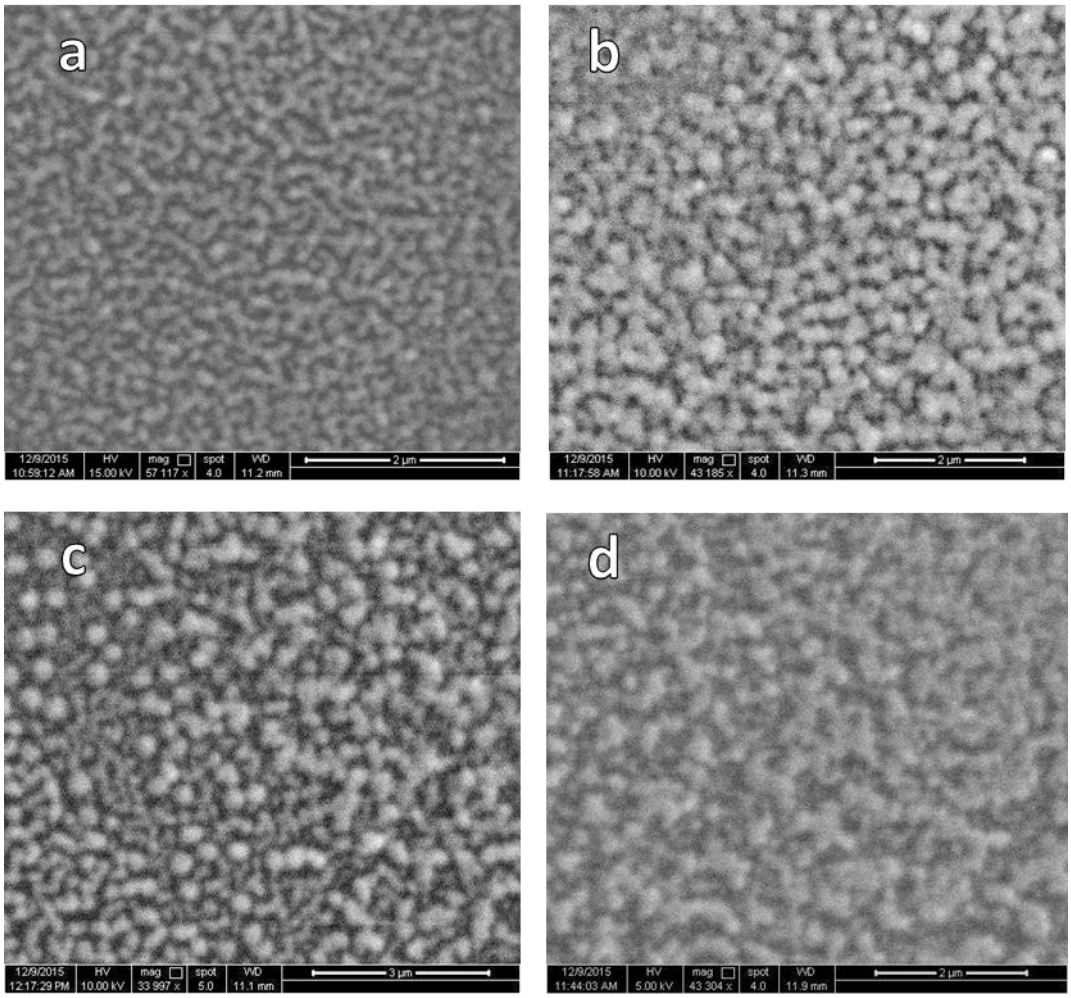

Fig.5: Surface morphology of Ag co-doped $Cd_{1-x}Cu_xO$ thin films obtained from SEM images analysis: (a) 0 % Ag (b) 4 % Ag (c) 6 % (d) 8 % Ag.

Figure (5a) shows the surface morphology and the surface microstructure of $Cd_{1-x}Cu_xO$ thin film, consists of spherical shaped grains uniformly distributed without detectable micro-cracks. As well as the grains is tightly packed and

agglomerations. Figures 5(b–d) shows the surface morphology of $Cd_{1-x}Cu_xO$ films co-doped with 4, 6, and 8 % of Ag molar ratio, respectively. Enhanced the surface uniformity and improved the distribution of the grain size with regular shapes can be notice in the Ag co-doped films. The EDXS spectrum shown in Fig. 6 reveals the presence of Cd, Cu, O and Ag peaks only, confirming again the purity of the prepared composition; the chemical composition is very close to the starting composition, see Fig. 6d. The EDXS measurement indicates that the deposited thin film is cadmium rich and is in a good agreement with the literature [26, 27, 31].

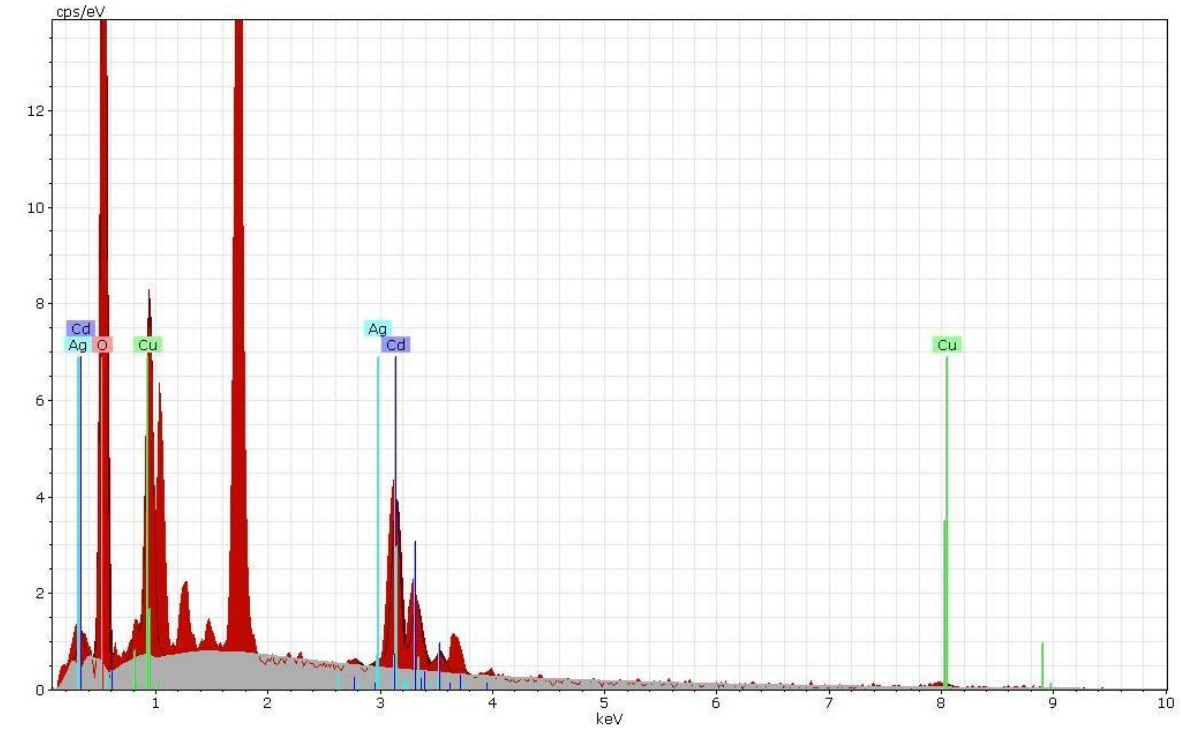

Spectrum: Acquisition

Element	Series	unn. C [wt.%]	norm. C [wt.%]	Atom. C [at.%]	Error (1 Sigma) [wt.%]
Oxygen	K-series	25.17	39.57	77.91	3.90
Copper	L-series	15.20	23.89	11.84	2.70
Cadmium	L-series	22.50	35.37	9.91	0.94
Silver	L-series	0.74	1.16	0.34	0.11
	Total:	63.60	100.00	100.00	

Fig. 6: EDXS spectrum of 6 % Ag co-doped $Cd_{1-x}Cu_xO$ thin films.

3.3 Surface topography (AFM analysis)

The surface topography and the grain size of the deposited thin films were studied using atomic force microscope (AFM). The roughness and the RMS roughness plays an important role in developing and characterize the optical properties for coating surface, moreover it gives an information about the surface quality under studying [27, 32]. Three dimensions surface topography of Ag co-doped $Cd_{1-x}Cu_xO$ thin films are represented in fig.7. AFM micrographs 2μm × 2μm were used to determination the surface roughness for these thin films. The figure shows the surface of all samples is uniform

and homogenous without any racks. The roughness of $Cd_{1-x}Cu_xO$ with x = 0.2 is 1.46 nm and slightly decrease to 0.77 nm for 4% Ag co-doped film. For 6% Ag co-doped $Cd_{1-x}Cu_xO$ roughness decreases to 1.3 nm whereas it is increased again to 4.24 nm for 8% Ag co-doping. Also the measured RMS roughness of 0,4,6 and 8% Ag co-doped $Cd_{1-x}Cu_xO$ thin films was 1.79, o.953, 1.58 and 4.99 nm respectively as illustrated in table 2. From fig. 7 it can be seen that the average grain size was slightly decrease from 94.3 for $Cd_{1-x}Cu_xO$ to 84.2 nm for 4% Ag co-doping then it was increase to 97.8 for 6% Ag co-doped film. Then it was decrease again to 83 nm for 8% Ag co-doped one. The measured values of roughness, RMS roughness and the average grain size are lower than those reported in literatures for doped and co-doped CdO thin films prepared by various techniques [8, 27, 32, 33, 34].

The variation of roughness, RMS roughness and the average grain size values clearly indicate that the Ag co-doping influences the surface topography of the deposited films and the quality of the thin film surface can be also controlled by the variation of the Ag co-doping concentration in the film, according to the AFM results.

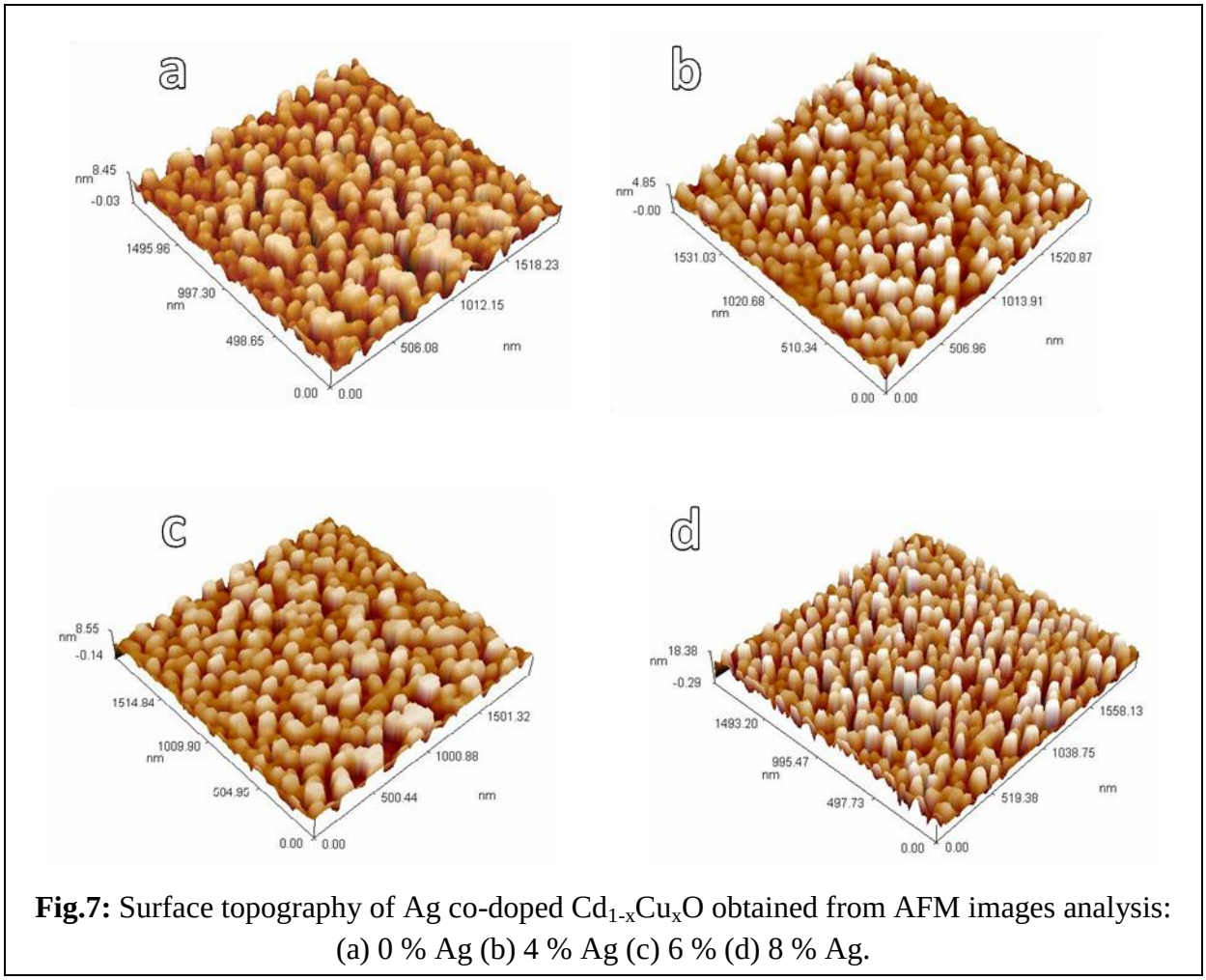

Fig.7: Surface topography of Ag co-doped $Cd_{1-x}Cu_xO$ obtained from AFM images analysis: (a) 0 % Ag (b) 4 % Ag (c) 6 % (d) 8 % Ag.

Table 2: The variation of the Roughness, Root Mean Square and the Average grain diameter of Ag co-doped $Cd_{1-x}Cu_xO$ thin films.

Sample	Roughness Average (nm)	Root Mean Square (nm)	Average grain diameter (nm)
$Cd_{1-x}Cu_xO$ X=0.2	1.46	1.79	94.3
$Cd_{1-x}Cu_xO$: Ag (4%)	0.779	0.953	84.2
$Cd_{1-x}Cu_xO$: Ag (6%)	1.3	1.58	97.8
$Cd_{1-x}Cu_xO$: Ag (8%)	4.24	4.99	83

3.4 Optical characteristics

The optical properties of solid materials depend on several parameters such as preparation conditions, the deposition technique, crystal structure, and surface topography, moreover their doping (ratio and type). The study of the fundamental absorption edge of semiconducting solid materials gives good and essential information about the electronic structure and the optical forbidden energy gap within the high energy a part of the optical absorption spectrum whereas the lower energy a part of the spectrum corresponds to the atomic vibrations [35, 36].Therefore the absorption edge of Ag co-doped $Cd_{1-x}Cu_xO$ should be studied here, fig.8 shows the absorbance and transmittance spectra as a function of incident photon wavelength for the different ratio of Ag co-doping films. It can be noticed from the figure that the absorbance and transmittance of the prepared films exhibit different behaviors in the visible and NIR regions, where the highest and lowest absorbance values were in the visible and NIR regions respectively. While the transmittance showed lower values about (20-60) % in the visible region and the high values about 80% in the NIR region. The Ag co-doped $Cd_{1-x}Cu_xO$ with 0-8% Ag/Cd ratios leads to increase the absorbance and decrease the transmittance in the visible region that is in agreement with the studies [3, 37, 38]. This can be attributed to the variation of the crystallinity of $Cd_{1-x}Cu_xO$ thin film by an occupation of Ag ions substitutional and interstitial sites in the $Cd_{1-x}Cu_xO$ lattice which lead to less crystallinity and increase the grain boundary leading to more light scattering and may be to the increased absorption by the free carriers [8, 34, 39].

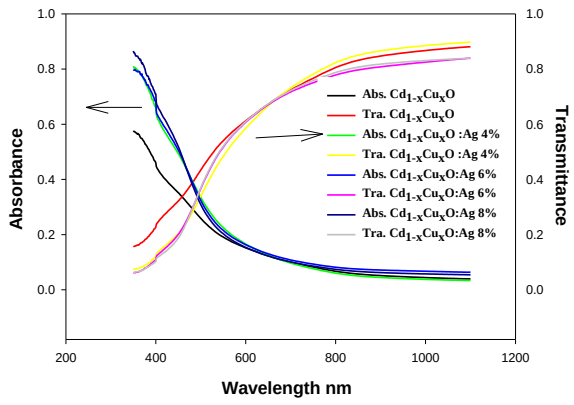

Fig.8: The absorbance and transmittance as a function of incident wavelength for Ag co-doped $Cd_{1-x}Cu_xO$ thin films.

The absorption coefficient (α) of deposited films can be determined using the following equation [40]:

$$\alpha = \frac{1}{t}\ln\left(\frac{1}{T}\right) \qquad (5)$$

where T is transmittance. The variation of the optical absorption coefficient with incident photon energy for different ratios of Ag co-doped $Cd_{1-x}Cu_xO$ thin films are shown in fig.9.

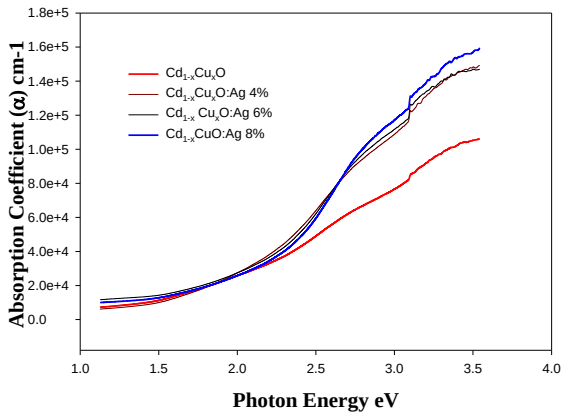

Fig.9: The optical absorption coefficient (α) as a function of incident photon energy of Ag co-doped $Cd_{1-x}Cu_xO$ thin films.

It is obvious from the figure that the value of absorption coefficient (α) increases with the increase of incident photon energy for all Ag co-doped $Cd_{1-x}Cu_xO$ prepared films. At the low energies in the NIR region the absorption coefficient value slightly increased, then it is rapidly increased in the visible and ultraviolet regions with the increasing the ratio of Ag content. This can be attributed to the absorbing nature of the Ag element. It can be noticed that the value of the absorption coefficient has high values in the order of 10^4 cm^{-1} for all samples which give an indicate that the electronic transitions were direct transitions.

The crystal structure, the arrangement, and distribution of atoms within the space lattice play an important role in the energy gap values of materials thin film samples. The values of the optical energy gap (E_g) can be determined from the relation between the absorption coefficient (α) and the incident photon energy (hν) using Tauc's relation [41,42]:

$$\alpha h\nu = \alpha_o (h\nu - E_g)^n \qquad (6)$$

Where α_o is an energy independent constant and called the band tailing parameter [35], E_g is the optical forbidden energy gap situated between the localized states near the mobility edges (Mott and Davis, 1971) [35, 43, 44]. n is constant called the power factor of the transition mode which depends on the nature of the material and the electronic transition. For direct allowed transition the value of n is (1/2), therefore the values of the optical energy gap of Ag co-doped $Cd_{1-x}Cu_xO$ thin films were determined from the plot of $(\alpha h\nu)^2$ versus the incident photon energy (hν) as shown in fig.10. From the extrapolation of the straight line portion to the hν axis at α = 0, the optical energy band gap E_g are obtained and the calculated values are tabulated in table 3. The E_g value for $Cd_{1-x}Cu_xO$ film was found to be 2.332 eV which matches with the values reported by A.A. Dakhel and R.K. Gupta et al. [4, 11]. It was observed that the absorption edge shifted toward higher energies and the optical energy gap increased to 2.406, 2.434 and 2.462 eV with increasing of Ag co-doping percentage 4%, 6% and 8% respectively, these values are adequately high for photovoltage and optoelectronic applications. The blue shift of absorption edge can be attributed to several reasons; (a) fundamental quantum size effect (quantum confinement) in nanostructured semiconductors [33, 34, 45, 46].]. It is reported that at small crystallite size.

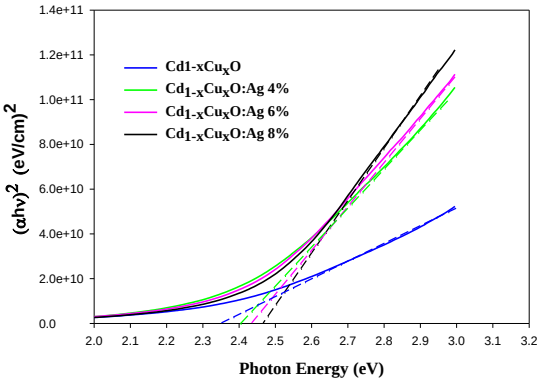

Fig.10: The plots of $(\alpha h\nu)^2$ Vs. hν For 0%, 4%, 6% and 8 % of Ag co-doped $Cd_{1-x}Cu_xO$ thin films.

the quantum confinement can be contributed to the widening of band gap [45,47]. The blue shift of the band gap E* is proportional to the radius of the particle R by the equation [48]:

$$E^* = E_g + \frac{\pi^2\hbar^2}{2R^2m^*} - \frac{1.8e^2}{\varepsilon R} \quad (7)$$

where E_g is the band gap in the bulk, ħ is the reduced Planck constant, e is the charge on the electron, m^* is the reduced mass of the electron and hole in the quantum region, and ε is the apparent dielectric constant of the semiconductor . It is obvious from eqn.7 that the blue shift in the band gap would occur if the size of the crystallite decreases.

With the increasing of Ag co-doping ratio, the crystallite size decreased and be smaller as in XRD results, where the band bending effect take place at the crystallite (grain) boundaries due to increase the surface to the volume ratio, which leads to widening of the optical band gap by the decreasing in the band bending. Similar results were reported by A.G. Imer [34], N. Manjul et al. [38] and R.K. Gupta et al. [45].

(b) Optical band gap blue shifted due to the band gap widening BGW or the Burstein–Moss effect [25, 22]. Where the increase in the carrier concentration by doping process will cause the Fermi level to move into the conduction band, and the filling of lower states in the conduction band by the electrons from the impurity atoms will results in a blue shift near the absorption band edge and then the electron need addition energy to transfer to the conduction band as reported by [37, 38, 42]. The widening of the optical band gap with the crystallite size and Ag co-doping concentration are illustrated in fig.11.

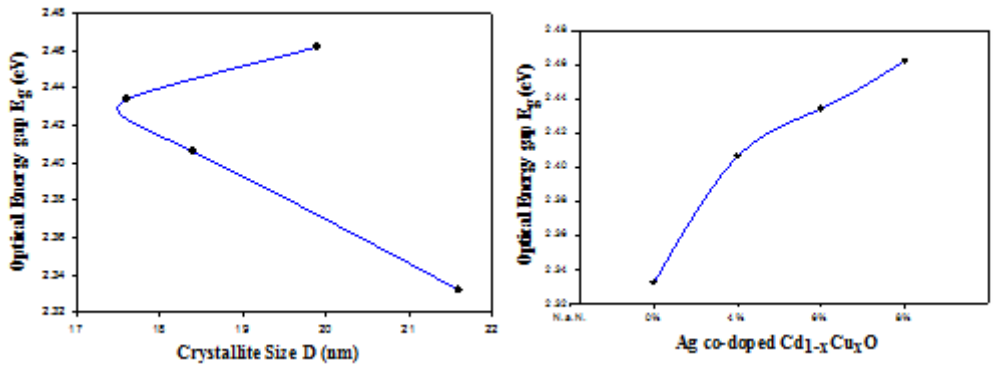

Fig.11: The variation of the optical energy gap with crytallite size and with Ag co-doping concentration.

In many amorphous and crystalline materials, absorption coefficient exponentially depends on the photon energy hν near the band edge. This part of the absorption coefficient curve called Urbach tail and characterizes local defects

which create localized states extended in the band gap for polycrystalline, low crystalline and amorphous materials [24,35] . The Urbach band tailing energy of the optical absorption edge in the material follows the empirical Urbach rule given by the equation [24, 38, 49]:

$$\alpha = \alpha_o \exp\left(\frac{h\nu}{E_U}\right) \rightarrow \ln\alpha = \ln\alpha_o + \frac{h\nu}{E_u} \quad \text{and} \quad E_U = \left[\frac{d\ln\alpha}{dh\nu}\right]^{-1} \qquad (8)$$

Where α_o is a constant, E_U is the band tail energy or Urbach energy.

The low crystallinity nature were absorbed in the Ag (0, 4, 6, 8)% co-doped $Cd_{1-x}Cu_xO$ thin films as shown in XRD pattern fig.1 and have been confirmed by the spectral behavior of the absorbance and absorption coefficient figs.8 and 9. The figures showed and confirmed that the prepared samples were verified Urbach rule and obey his empirical equation (8).The figures also reveal that there are a tail region for $Cd_{1-x}Cu_xO$ and Ag co-doped $Cd_{1-x}Cu_xO$ samples. Similar behavior was reported for low crystallinity semiconductors in the literature [24, 35, 36, 38, 42]. The variation of ln (α) versus photon energy (hν) for Ag (0, 4, 6, 8)% co-doped $Cd_{1-x}Cu_xO$ thin films are shown in fig.12. The Urbach energy values were estimated from the slopes of the plots inset of Fig. 12, and the values are illustrated in Table 3. The Urbach energy values for Ag (0, 4, 6, 8)% co-doped $Cd_{1-x}Cu_xO$ are 0.839 , 0.696, 0.690 and 0.616 eV respectively, where the band tails energy E_U values decreased with increasing of Ag dopant concentration as shown in fig.13a. This can relate to the minimization of the number of crystal defects and enhancement of the quality of the co-doped films and this may be the reason for increased the energy gap of these films. Fig.13b shows the variation of band tails energy E_U versus the values of optical energy gap E_g of Ag co-doping $Cd_{1-x}Cu_xO$ thin films.

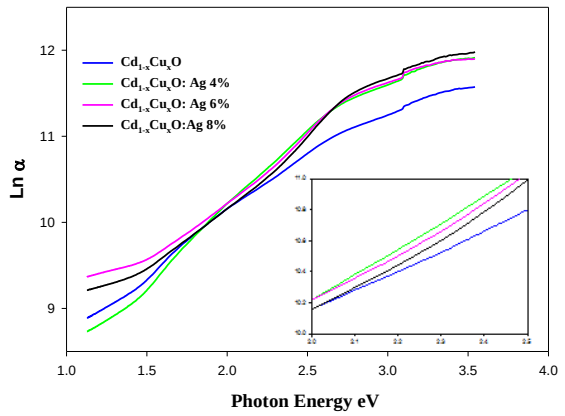

Fig.12: Variation of ln (α) with energy (hν) for Ag (0, 4, 6, 8)% co-doped $Cd_{1-x}Cu_xO$ thin films, from which Urbach energy can be obtained.

Table 3: The values of the optical band gap energy (Eg), the band tail width (E_U) Urbach energy of Ag co-doped $Cd_{1-x}Cu_xO$ thin films.

Sample	Wavelength of absorption edge (nm)	E_g (eV)	E_u (eV)
$Cd_{1-x}Cu_xO$	531.73	2.332	0.839
$Cd_{1-x}Cu_xO$:Ag 4%	515.37	2.406	0.696
$Cd_{1-x}Cu_xO$:Ag 6%	509.44	2.434	0.690
$Cd_{1-x}Cu_xO$:Ag 8%	503.65	2.462	0.616

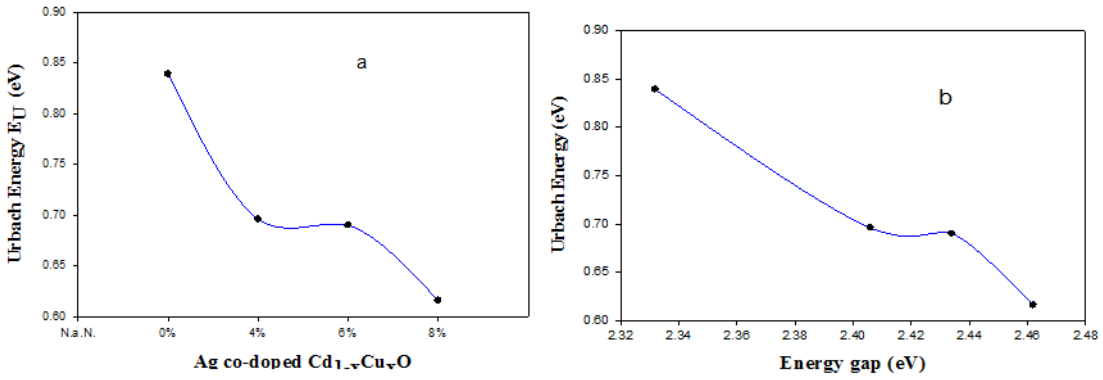

Fig.13: (a) E_U as a function of Ag co-doping content, (b) E_U Vs. optical energy gap of Ag co-doped $Cd_{1-x}Cu_xO$ thin films.

4. Conclusions

In the present work $Cd_{1-x}Cu_xO$ and Ag co-doped $Cd_{1-x}Cu_xO$ Nanostructured thin films *have been successfully deposited on glass substrates at constant temperature of 350 ^oC by* chemical spray pyrolysis technique. The Ag co-doping with different Ag content was performed on the $Cd_{1-x}Cu_xO$ with x=0.2 thin film to enhance its structural and optical properties to be more suitable photovoltage and optoelectronic applications. The XRD results revealed that all prepared films was polycrystalline structure and have low crystalline nature. The crystallite size for the preferred orientation (111) was decreased from 21.59 nm to 19.86 nm with increase of Ag co-doping level. Increased of dislocation density and micro-strain were obtained with increase of Ag content , the small values of dislocation density confirms that the spray pyrolysis is an effective technique and can be used to deposit good and high quality Ag co-doped $Cd_{1-x}Cu_xO$ thin films. Surface morphology and surface topography got improved and can be controlled by Ag co-doping. The optical properties studied show that, the prepared films have high absorbance and high transmittance (more than 80%) in the visible and near infrared regions respectively with high absorption coefficient α of the order 10^4 cm^{-1}. The values of the optical energy gap for direct allowed transitions were found to be blue shifted from 2.332 eV to 2.462 eV with increasing of Ag co-doping content. This is due to quantum size effect and B.M effect. The band tail width (EU), or Urbach energy, was found to be decreased with the increase of Ag co-doping content. The widened optical band gap and decreased band tail width make Ag co-doped $Cd_{1-x}Cu_xO$ films more suitable for photovoltaic and optoelectronic applications such as in solar cells.

Acknowledgement

The author thank Mr. Salah M. Saleh and Eqbal Abduljalil Mahdi for the UV–vis and XRD measurements..

5. Reference

[1] N. Thovhogi , E. Park , E. Manikandan , M. Maaza and A. Gurib-Fakim, Journal of Alloys and Compounds, 655, (2016) ,314-320.

[2] A.A.Dakhela, M.Bououdina , Mater.Sci.Semicond.Process,26 ,(2014), 527-532.

[3] M. Yüksel , B. Şahin, F. Bayansal, Ceramics International, 42, 5, (2016), 6010–6014.

[4] A.A. Dakhel ,Solid State Sciences , 31,(2014),1-7.

[5] B. Hymavathi, B. Rajesh Kumar and T. Subba Rao, Procedia Materials Science, 10, (2015), 285 – 291.

[6] K. Sankarasubramanian , P. Soundarrajan , K. Sethuraman and K. Ramamurthi, Mater.Sci.Semicond.Process, 40 ,(2015), 879-884.

[7] S.ukru Karatas and F. Yakuphanoglu, Journal of Alloys and Compounds, 537,(2012), 6–11.

[8] R.K. Guptaa, Z. Serbetc and F. Yakuphanoglu, Journal of Alloys and Compounds,515,(2012),96-100.

[9] Zhao-Qing Liu, Rui Guo, Gao-Ren Li, Qiong Bua, Wen-Xia Zhaoc and Ye-Xiang Tonga, Electrochimica Acta,59, (2012), 449– 454.

[10] M. Zaien, A. Hmood, N.M. Ahmed and Z. Hassan, Materials Letters ,102-103 ,(2013), 12-14.

[11] Zheng Biju and Hu Wen, Journal of Semiconductors, 34, 5, (2013), 053003-1-4.

[12] L.R. de León-Gutiérrez , J.J. Cayente-Romero , J.M. Peza-Tapia , E. Barrera Calva, J.C. Martínez-Flores and M. Ortega-López, Materials Letters, 60, (2006), 3866–3870.

[13] D.S. Dhawale, A.M. More, S.S. Latthe, K.Y. Rajpure and C.D. Lokhande, Applied Surface Science , 254, (2008), 3269–3273.

[14] S. J. Helen, Suganthi Devadason and T. Mahalingam , J Mater Sci: Mater Electron, 27, 5, (2016), 4426-4432.

[15] A.D. Shannon, Acta. Cryst.,A32,(1976), 751- 767. Acta

[16] A.A. Dakhel, Thin Solid Films, 518, (2010), 1712–1715.

[17] R.J. Deokate, S.M. Pawar, A.V. Moholkar, V.S. Sawant, C.A. Pawar, C.H. Bhosale, K.Y. Rajpure, Appl. Surf. Sci., 254, (2008), 2187-2195.

[18] B. Saha, S. Das, K.K. Chattopadhyay, Sol. Energy Mater. Sol. Cells 91 (2007) 1692-1697.

[19] A. Salem , Eur. Phys. J. Plus, 129, (2014), 263-274.

[20] X B Wang, C Song, K W Geng, F Zeng and F Pan, J. Phys. D: Appl. Phys. 39 (2006) 4992–4996.

[21] A. A. Dakhel and M. Bououdina, Appl. Phys. A (2015) 119:1053–1060.

[22]

[23] Y. Gulen , B. Sahin , F. Bayansal and H.A. Cetinkara, Superlattices and Microstructures 68 (2014) 48–55.

[24] Adel H. Omran Alkhayatt, Sabah M. Thahab and Inass Abdulah Zgair, Optik 127, (2016), 3745–3749.

[25] Adel H. Omran Alkhayatt and Shymaa K. Hussian, Materials Letters, 155, (2015), 109–113.

[26] P. Velusamy, R. Ramesh Babu, K. Ramamurthi, J. Viegas and E. Elangovan, J Mater Sci: Mater Electron, (2015), 26,4152–4164.

[27] P.Velusamy, R.RameshBabu, K.Ramamurthi, E.Elangovan, J.Viegas, M.S. Dahlem and M.Arivanandhan, Ceramics International, 42, (2016), 12675–12685.

[28] M. Dongol, A. El-Denglawey, M.S. Abd El Sadek and I.S. Yahia, Optik 126 (2015) 1352–1357.

[29] M.M. El-Nahass, Z. El-Gohary and H.S. Soliman, Optics & Laser Technology 35, (2003) 523 – 531.

[30] S. Sen, S.K. Halder, S.P. Sen Gupta, J. Phys. Soc. Japan. 38, 6, (1975), 1641-1647.

[31] B. Saha, R. Thapa and K.K. Chattopadhyay, Solid State Communications, 145, (2008), 33–37.

[32] A. Abdolahzadeh Ziabari, F.E. Ghodsi and G. Kiriakidis, Surface & Coatings Technology 213, (2012), 15–20.

[33] B. Sahin and F. Bayansal, Facile synthesis of group-I elements (K, Li and Na)-doped nanostructured CdO films, Philosophical Magazine, 03, 54, (2014) , 1-13.

[34] Arife Gencer Imer, Superlattices and Microstructures, 92, (2016), 278-284.

[35] A.S. Hassanien and Alaa A. Akl, Superlattices and Microstructures, 89, (2016), 153-169.

[36] M. El-Hagary, M.Emam-Ismail, E.R.Shaaban and A.El-Taher, Radiation Physics and Chemistry, 81, (2012), 1572–1577.

[37] K. Usharani, A. R. Balu and V. S. Nagarethinam, Surface Engineering, 32,11 , (2016), 829-833.

[38] N. Manjula, A.R. Balu, K. Usharani, N. Raja and V.S. Nagarethinam, Optik, 127, (2016) 6400–6406.

[39] A.V. Moholkara, G.L. Agawane, Kyu-Ung Sim, Ye-bin Kwon, K.Y. Rajpure and J.H. Kim, Applied Surface Science, 257, (2010), 93–101.

[40] M. Thirumoorthi and J. Thomas Joseph Prakash, Journal of Asian Ceramic Societies, 4, (2016), 39–45.

[41] J. Tauc, Amorphous and Liquid Semiconductors, Plenum, New York, 1974.

[42] Seckin Akın , Gamze Karanfil , Aytac Gultekin and Savas Sonmezoglu, Journal of Alloys and Compounds, 579, (2013), 272–278.

[43] N.F. Mott, E.A. Davis, Electronic Processes in Non-crystalline Materials, Clarendon Press, Oxford, 1979.

[44] K.A. Aly, A.M. Abd Elnaeim, N. Afify, A.M. Abousehly, J. Non Cryst. Solids 358 (2012) 2759.

[45] R.K. Gupta, F.Yakuphanoglu and F.M. Amanullah, Physica E, 43, (2011), 1666–1668.

[46] B. Sahin, F.Bayansal, M.Yuksel, N.Biyikli and H.A.Çetinkara, Ceramics International, 40, (2014), 5237–5243.

[47] M. Green and Z. Hussain, J. Appl. Phys. 69, (ll), (1991), 7788-7796.

[48] N. Satoh, T. Nakashima, K. Kamikura and K. Yamamoto, Nat. Nanotechnol., 3, (2008), 106-111.

[49] F. Urbach, Phys. Rev., 92, (1953), 1324.